An International Journal of Optimization and Control: Theories & Applications
ISSN: 2146-0957 eISSN: 2146-5703
Vol.15, No.3, pp.535-548 (2025)
https://doi.org/10.36922/IJOCTA025110048

RESEARCH ARTICLE

A numerical method for solving distributed-order multi-term time-fractional telegraph equations involving Caputo and Riesz fractional derivatives

Safar Irandoust Pakchin[1*], Mohammad Hossein Derakhshan[1], and Shahram Rezapour[2,3*]

[1]Department of Applied Mathematics, Faculty of Mathematics, Statistics and Computer Sciences, University of Tabriz, Tabriz, East Azerbaijan, Iran
[2]Department of Mathematics, Faculty of Basic Sciences, Azarbaijan Shahid Madani University, Tabriz, East Azerbaijan, Iran
[3]Department of Medical Research, China Medical University Hospital, China Medical University, Taichung, Taiwan
s.irandoust@tabrizu.ac.ir, m.h.derakhshan.20@gmail.com, sh.rezapour@azaruniv.ac.ir

ARTICLE INFO

Article History:
Received: March 10, 2025
Revised: April 27, 2025
Accepted: April 30, 2025
Published Online: July 23, 2025

Keywords:
Distributed-order
Finite difference method
Fractional derivative
Riesz fractional derivative
Stability analysis
Telegraph equations

Subject Classification:
26A33; 65M06; 65M12; 35R11; 47B06; 65R20

ABSTRACT

This paper introduces a robust distributed-order time-fractional telegraph model, incorporating Caputo time- and Riesz space-fractional derivatives. The spatial Riesz derivative is discretized using an optimized finite difference method. For the distributed-order fractional operator, the midpoint rule was first used to approximate the integral with respect to the order distribution, followed by the application of a finite difference scheme to approximate the Caputo time-fractional derivative. The method's flexibility and high accuracy make it a valuable tool for modeling and simulating these systems, providing insights into the behavior of fractional-order systems with both temporal and spatial fractional effects. Additionally, the proposed approach outperforms existing numerical methods in terms of both precision and computational efficiency, making it highly applicable for real-world problems requiring accurate and efficient solutions. A comprehensive analysis of convergence and stability was conducted to validate the proposed numerical method. To demonstrate its effectiveness, several numerical simulations were performed, revealing the method's exceptional accuracy and computational efficiency. Furthermore, a comparison with existing numerical approaches from the literature is provided, highlighting the proposed method's superior performance in both precision and practical applicability.

1. Introduction

Over the past few decades, there has been growing interest among researchers in modeling and analyzing complex physical phenomena using fractional-order operators, particularly in the fields of mathematical sciences and engineering.[1–7] The significant advantage of fractional models, viewed as generalizations of classical integer-order models, lies in their ability to more accurately capture anomalous transport processes, especially those involving memory effects and spatial heterogeneity.[8–15] Many complex physical systems, such as diffusion in multifractal media, cannot be effectively described by single-order differential equations. Therefore, it becomes essential to explore fractional-order and, particularly, distributed-order differential models to account for the inherent complexities of such phenomena. The study of distributed-order time-fractional models began

*Corresponding Author

with Caputo,[16] who investigated their application in describing stress–strain relationships in viscoelastic media. Subsequently, Caputo further expanded on these models to include applications in dielectric relaxation and anomalous diffusion phenomena.[17,18] Building upon this foundation, Chechkin et al.[19] introduced and analyzed distributed-order time-fractional models in greater depth, further highlighting their effectiveness in representing physical systems that exhibit a broad spectrum of dynamical behaviors.

Sokolov et al.[20] studied and introduced distributed-order time-fractional models, also referred to as diffusion-like models, to provide a kinetic interpretation of anomalous diffusion and to describe relaxation phenomena.[21–24] Among these models, the fractional telegraph equation has garnered significant attention due to its versatility in modeling various physical and mathematical phenomena. It has been effectively used in the study of diffusive processes, elastic manifold structures, and wave-like anomalous behaviors. Furthermore, this class of equations has a broad application across different fields, including mathematical sciences, engineering, and physics.[25–27] The classical time-fractional diffusion-wave model of distributed order can be extended to the distributed-order time-fractional telegraph model by simultaneously considering the fractional derivatives of distributed order over the intervals (0,1) and (1,2). This formulation allows for a more comprehensive description of systems that exhibit both diffusive and wave-like characteristics, capturing a wider range of dynamic behaviors observed in complex media.

Obtaining analytical solutions for distributed-order fractional models is often a challenging task due to the complexity of the underlying operators and the nonlocal nature of fractional derivatives. Consequently, numerical methods have become essential tools for solving such models effectively. A wide range of numerical techniques has been developed in the literature, each tailored to specific types of fractional equations and boundary conditions. These include different schemes,[28,29] the fractional-centered difference method,[30] fast second-order implicit difference methods,[31] and Petrov–Galerkin as well as spectral collocation techniques.[32] Other methods, such as direction implicit difference approaches,[33] the operational matrix method,[34] and hybrid function-based techniques[35] have also been explored. Additionally, meshless methods,[36] compact difference schemes,[37] and finite difference-spectral methods[38] offer alternative strategies. More advanced frameworks, such as the alternating direction implicit-Galerkin finite element method,[39] finite element approximations,[40] and the shifted fractional Jacobi spectral algorithm[41] have further expanded the toolbox for solving these models. Some studies have combined the finite difference method with the matrix transfer technique to handle the space-fractional derivative in distributed-order models,[42] while others have employed the shifted Legendre method[43] or introduced novel matrix representations of fractional models.[44] Collectively, these methods reflect the rich and diverse landscape of numerical strategies developed to tackle the inherent difficulties in distributed-order fractional differential equations.

In this work, we propose an efficient and high-performance numerical method for solving the distributed-order time-fractional telegraph model, formulated as follows in Equation (1):

$$\int_0^1 b_1(\mu)\,{}^C D_t^{\mu} u d\mu + \int_1^2 b_2(\nu)\,{}^C D_t^{\nu} u d\nu = \mathbb{H}(x,t,u) \tag{1}$$

in which $\mathbb{H}(x,t,u) = -\kappa(-\Delta)^{\frac{\alpha}{2}}u + f(x,t,u)$, subject to the initial and boundary conditions in Equation (2):

$$\begin{aligned} &u(x,0) = \psi(x),\ 0 \le x \le L, \\ &u(0,t) = \varphi_0(t),\ u(L,t) = \varphi_L(t)\ 0 < t \le T \end{aligned} \tag{2}$$

Here, $\mu \in (0,1]$, $\nu \in (1,2]$, and ${}^C D_t^{\mu}$, ${}^C D_t^{\nu}$ are defined as in Equation (3):

$$\begin{aligned} &{}^C D_t^{\beta} u(x,t) = (\Gamma(n-\beta))^{-1} \\ &\times \int_0^t u^{(n)}(x,\tau)\frac{1}{(t-\tau)^{\beta-n+1}}d\tau, \\ &n-1 < \beta \le n,\ n \in \mathbb{N} \end{aligned} \tag{3}$$

Here, $-(-\Delta)^{\frac{\alpha}{2}}u$ denotes the Riesz fractional operator in Equation (4)

$$-(-\Delta)^{\frac{\alpha}{2}}u = C_\alpha({}_x D_+^{\alpha}u + {}_x D_-^{\alpha}u) \tag{4}$$

in which $c_\alpha = -\frac{1}{2\cos(\frac{\pi\alpha}{2})}$, and ${}_x D_+^{\alpha}$, ${}_x D_-^{\alpha}$ are displayed by Equation (5)[34]:

$$\begin{aligned} &{}_x D_+^{\alpha} u(x,t) = \frac{d^2}{dx^2}({}_x \mathbb{I}_+^{2-\alpha} u(x,t)) \\ &= \frac{u(a,t)}{\Gamma(1-\alpha)(x-a)^{\alpha}} + \frac{u'(a,t)}{\Gamma(2-\alpha)(x-a)^{\alpha-1}} \\ &+ \frac{1}{\Gamma(2-\alpha)}\int_a^x u^{(2)}\frac{1}{(\xi,t)(x-\xi)^{\alpha-1}}d\xi \end{aligned} \tag{5}$$

and Equation (6):

$$
\begin{aligned}
&{}_xD_-^{\alpha}u(x,t) = \frac{d^2}{dx^2}({}_x\mathbb{I}_-^{2-\alpha}u(x,t)) \\
&= \frac{u(b,t)}{\Gamma(1-\alpha)(b-x)^{\alpha}} - \frac{u'(b,t)}{\Gamma(2-\alpha)(b-x)^{\alpha-1}} \\
&+ \frac{1}{\Gamma(2-\alpha)}\int_x^b u^{(2)}(\xi,t)\frac{1}{(\xi-x)^{\alpha-1}}d\xi
\end{aligned} \tag{6}
$$

where ${}_x\mathbb{I}_+$ and ${}_x\mathbb{I}_-$ are as defined by Ahmed and Hashem.[44] This class of fractional differential equations is characterized by the incorporation of distributed-order derivatives, which allow for a more nuanced modeling of memory and hereditary properties inherent in complex physical and engineering systems. Specifically, the model under investigation incorporates time-fractional derivatives of distributed order in the Caputo sense, which are particularly advantageous for initial value problems due to their physically interpretable initial conditions.

To numerically solve the equation introduced above, the combined approach of the midpoint method and finite differences was used. To estimate the integral term, we applied the midpoint method and then used the finite differences method to approximate the Caputo fractional operator in the time direction. For the Riesz space-fractional derivative with respect to the space variable, we used the finite difference approach.[45] The implications of the proposed method are significant in solving complex distributed-order multi-term time-fractional telegraph equations, which are commonly encountered in various scientific and engineering fields. These equations arise in phenomena such as anomalous diffusion, wave propagation in heterogeneous media, and modeling complex materials with memory effects. In this paper, we introduced a novel numerical method for solving the distributed-order time-fractional telegraph model, which incorporates Caputo time derivatives and Riesz space-fractional derivatives. The primary contribution of this work lies in the development of a robust and efficient numerical scheme that combines an optimized finite difference method for the spatial Riesz derivative and a midpoint rule for discretizing the integral in the distributed-order fractional operator. This approach is followed by a finite difference scheme to approximate the Caputo time-fractional derivative. The novelty of the proposed method lies in its ability to accurately handle the complexity of the distributed-order and multi-term fractional operators simultaneously, ensuring both high accuracy and computational efficiency. To the best of our knowledge, this is one of the first approaches that directly addresses the challenges of solving such equations with both spatial and temporal fractional derivatives in a unified framework. We also provide a comprehensive analysis of the method's convergence and stability, establishing its robustness for practical applications. Several numerical experiments are conducted to demonstrate the effectiveness of the method in solving real-world problems. The proposed approach is then benchmarked against existing numerical methods in the literature, highlighting its superior performance in terms of both precision and computational efficiency. This method has broad implications for applications in fields such as anomalous diffusion, wave propagation in heterogeneous media, and modeling of complex materials with memory effects, where distributed-order time-fractional equations play a key role in accurately describing underlying physical processes.

In Section 2, we present a numerical approach based on finite differences for approximating the Caputo fractional operator. In Section 3, we introduce an implicit numerical method for approximating the solution to Equation (1). Section 4 provides the convergence and stability analyses of the proposed numerical method, ensuring its reliability. In Section 5, we present several numerical examples to validate the efficiency and effectiveness of the proposed method. Finally, Section 6 offers the concluding remarks, summarizing the key findings and potential future directions.

2. A description of the numerical approach for the fractional operator

Suppose that $\Delta t = \frac{b-a}{N}$, $t = t_k = a + k\Delta t$, $u^0 = u(x,a) = u(x,t-k\Delta t), u^1 = u(x,a+\Delta t) = u\left(x,t-(k-1)\Delta t\right),\ldots,u^{k-j} = u(x,t-j\Delta t),\ldots,$ *and* $u^k = u(x,t) = u(x,a+k\Delta t)$, then it can be presented as in Equation (7):

$$
\begin{aligned}
D_t^{\nu}u(x,t_k) &= \frac{1}{\Gamma(2-\nu)}\int_a^t u^{(2)}(x,\tau)(t-\tau)^{1-\nu}d\tau \\
&= \frac{1}{\Gamma(2-\nu)}\int_0^{t-a} u^{(2)}(x,t-\tau)\tau^{1-\nu}d\tau \\
&= \frac{1}{\Gamma(2-\nu)}\sum_{j=0}^{k-1}\int_{j\Delta t}^{(j+1)\Delta t} u^{(2)}(x,t-\tau)\tau^{1-\nu}d\tau \\
&= \frac{(\Delta t)^{-2}}{\Gamma(2-\nu)}\sum_{j=0}^{k-1}(u(x,t+k_1)-2u(x,t+k_2) \\
&\quad + u(x,t+k_3)\int_{j\Delta t}^{(j+1)\Delta t}\frac{1}{\tau^{\nu-1}}d\tau
\end{aligned}
$$

$$= \frac{(\Delta t)^{-\nu}}{\Gamma(3-\nu)} \sum_{j=0}^{k-1} b_j^{\nu} (u(x, t_{k-j+1}) - 2u(x, t_{k-j}) + u(x, t_{k-j-1})) \tag{7}$$

in which $k_1 = (1-j)\Delta t$, $k_2 = -j\Delta t$, $k_3 = (-j-1)\Delta t$ and $b_j^{\nu} = ((j+1)^{2-\nu} - j^{2-\nu})$.

Also, by applying a similar technique, we get Equation (8):

$$\begin{aligned} D_t^{\mu} u(x,t) &= \frac{1}{\Gamma(1-\mu)} \int_a^t u^{'}(x,\tau)(t-\tau)^{-\mu} d\tau \\ &= \frac{1}{\Gamma(1-\mu)} \int_0^{t-a} u^{'}(x, t-\tau)\tau^{-\mu} d\tau \\ &= \frac{1}{\Gamma(1-\mu)} \sum_{j=0}^{k-1} \int_{j\Delta t}^{(j+1)\Delta t} u^{'}(x, t-\tau)\tau^{-\mu} d\tau \\ &= \frac{1}{\Gamma(1-\mu)} \sum_{j=0}^{k-1} \frac{u(x, t+k_1) - u(x, t+k_2)}{\Delta t} \\ &\quad \times \int_{j\Delta t}^{(j+1)\Delta t} \frac{1}{\tau^{\mu}} d\tau \\ &= \frac{(\Delta t)^{-\mu}}{\Gamma(2-\mu)} \sum_{j=0}^{k-1} b_j^{\mu} (u(x, t_{k-j+1}) - u(x, t_{k-j})) \end{aligned} \tag{8}$$

in which $b_j^{\mu} = ((j+1)^{2-\mu} - j^{2-\mu})$. For $1 < \alpha < 2$, the Riesz fractional operator can be estimated as in Equation (9)[45]:

$$\begin{aligned} &-(-\Delta)^{\alpha/2} u(x,t) = -\frac{(\Delta x)^{-\alpha}}{2\Gamma(\alpha)\Gamma(3-\alpha)\cos\left(\frac{\pi\alpha}{2}\right)} \\ &\times \left\{ \frac{(1-\alpha)(2-\alpha)u_0}{q^{\alpha}} + \frac{(2-\alpha)}{q^{\alpha-1}}(u_1 - u_0) \right. \\ &+ \sum_{i=0}^{q-1} (u_{q-i+1} - 2u_{q-i} + u_{q-i-1}) \left[(i+1)^{2-\alpha} - i^{2-\alpha}\right] \\ &+ \frac{(1-\alpha)(2-\alpha)u_M}{(M-q)^{\alpha}} - \frac{(2-\alpha)}{(M-q)^{\alpha-1}}(u_M - u_{M-1}) \\ &\left. + \sum_{i=0}^{M-q-1} (u_{q+i-1} - 2u_{q+i} + u_{q+i+1}) \left[(i+1)^{2-\alpha} - i^{2-\alpha}\right] \right\} \end{aligned} \tag{9}$$

in which $\Delta x = \frac{b-a}{M}$, $x = x_q = a + q\Delta x$, $u_0 = u(a,t) = u(x - q\Delta x, t), u_1 = u(a + \Delta x, t) = u(x - (q-1)\Delta x, t), \ldots, u_{q-i} = u(x - i\Delta x, t), \ldots, u_q = u(x,t) = u(a + q\Delta x, t)$

3. Description of the numerical method

In this section, we present the discretization method used for approximating the integral terms in the distributed-order fractional operator. The proposed method utilized a quadrature rule to evaluate these integrals. This choice was motivated by the fact that quadrature methods provide a flexible and accurate approach to numerical integration, especially when dealing with functions that are difficult to handle analytically. Furthermore, quadrature methods are widely used for handling fractional integrals due to their ability to approximate the integrals over complex domains with high precision. Therefore, we have Equation (10):

$$\int_a^b b(\gamma)\, {}^{C}D_t^{\gamma} u(x,t) d\gamma = h \sum_{p=0}^{L} b(\gamma_p)\, {}^{C}D_t^{\gamma_p} u(x,t) - \frac{h^2}{24} F''(\gamma),\ \gamma \in (a,b) \tag{10}$$

where $\gamma_p = \frac{\eta_{p-1} + \eta_p}{2}$, $p = 1, \ldots, L$, $\gamma_p \in [\eta_{p-1}, \eta_p]$, and the interval $[\eta_{p-1}, \eta_p]$ is a partition of the L subintervals of $[a,b]$ with equal amplitude $h = \frac{b-a}{L}$. Here F is $F = b(\gamma)\, {}^{C}D_t^{\gamma} u(x,t)$.

Then, using Equation (10), we have Equation (11):

$$\int_0^1 b_1(\mu)\, {}^{C}D_t^{\mu} u(x,t) d\mu = \frac{1}{L} \sum_{p=0}^{L} b_1(\mu_p)\, {}^{C}D_t^{\mu_p} u(x,t) - \frac{h^2}{24} F''_1(\mu),\ \mu \in (0,1) \tag{11}$$

where $\mu_p = \frac{\eta_{p-1} + \eta_p}{2}$ for $p = 1, \ldots, L$. We consider the interval $[\eta_{p-1}, \eta_p]$ with equal amplitude $h = \frac{b-a}{L}$ such that $[\eta_{p-1}, \eta_p] \subseteq [0,1]$, $F_1 = b_1(\mu)\, {}^{C}D_t^{\mu} u(x,t)$. Similar to the procedures in Equation (11), we have Equation (12):

$$\int_1^2 b_2(\nu)\, {}^{C}D_t^{\nu} u(x,t) d\nu = \frac{1}{L} \sum_{p=0}^{L} b_2(\nu_p)\, {}^{C}D_t^{\nu_p} u(x,t) - \frac{h^2}{24} F''_2(\nu),\ \nu \in (1,2) \tag{12}$$

where $\nu_p = \frac{\eta'_{p-1} + \eta'_p}{2}$ for $p = 1, \ldots, L$ and considering the interval $[\eta'_{p-1}, \eta'_p]$ with equal amplitude $h = \frac{b-a}{L}$ such that $[\eta'_{p-1}, \eta'_p] \subseteq [1,2]$ and $F_2 = b_2(\nu)\, {}^{C}D_t^{\nu} u(x,t)$

Neglecting $\circ(h^2)$ in Equations (11) and (12), Equation (1) can be approximated as Equation (13):

$$\frac{1}{L} \sum_{p=0}^{L} b_1(\mu_p)\, {}^{C}D_t^{\mu_p} u(x,t) + \frac{1}{L} \sum_{p=0}^{L} b_2(\nu_p)\, {}^{C}D_t^{\nu_p} u(x,t) = -\kappa(-\Delta)^{\frac{\alpha}{2}} u(x,t) + f(x,t,u(x,t)) \tag{13}$$

By putting ${}^{C}D_t^{\mu_p}u(x,t)$, ${}^{C}D_t^{\nu_p}u(x,t)$, and $-(-\Delta)^{\frac{\alpha}{2}}u(x,t)$ into Equation (1), and showing by $U_q^k \approx u(x_q,t_k)$, we acquire Equation (14):

$$\begin{aligned}
&\frac{1}{L}\sum_{p=0}^{L} b_1(\mu_p)\left(\frac{(\Delta t)^{-\mu_p}}{\Gamma(2-\mu_p)}\sum_{j=0}^{k-1}(U_q^{k-j+1}-U_q^{k-j})\right)\\
&\times((j+1)^{1-\mu_p}-j^{1-\mu_p}))+\frac{1}{L}\sum_{p=0}^{L} b_2(\nu_p)\left(\frac{(\Delta t)^{-\nu_p}}{\Gamma(3-\nu_p)}\right.\\
&\times\sum_{j=0}^{k-1}(U_q^{k-j+1}-2U_q^{k-j}+U_q^{k-j-1})((j+1)^{2-\nu_p}-j^{2-\nu_p}))\\
&=-\frac{\kappa(\Delta x)^{-\alpha}}{2\Gamma(\alpha)\Gamma(3-\alpha)\cos(\frac{\pi\alpha}{2})}\left\{\frac{(1-\alpha)(2-\alpha)U_0^k}{q^\alpha}\right.\\
&+\frac{(2-\alpha)}{q^{\alpha-1}}(U_1^k-U_0^k)+\sum_{i=0}^{q-1}(U_{q-i+1}^k-2U_{q-i}^k\\
&+U_{q-i-1}^k)[(i+1)^{2-\alpha}-i^{2-\alpha}]+\frac{(1-\alpha)(2-\alpha)U_M^k}{(M-q)^\alpha}\\
&-\frac{(2-\alpha)}{(M-q)^{\alpha-1}}(U_M^k-U_{M-1}^k)+\sum_{i=0}^{M-q-1}(U_{q+i-1}^k-2U_{q+i}^k\\
&\left.+U_{q+i+1}^k)[(i+1)^{2-\alpha}-i^{2-\alpha}]\right\}+f(x_q,t_k,U_q^k)
\end{aligned}\tag{14}$$

under the conditions as in Equation (15):

$$\begin{aligned}
&U_q^0=\psi(q\Delta x),\ q=0,1,\ldots,M,\\
&U_0^k=\varphi_0(k\Delta t),\ U_M^k=\varphi_L(k\Delta t)\ k=0,1,\ldots,N
\end{aligned}\tag{15}$$

4. Convergence and stability

The stability analysis, along with convergence, is obtained by the proposed numerical method, which is presented in **Section 3**. For simplicity, we can rewrite Equation (14) as follows in Equation (16):

$$T_1(U_q^{k+1})=T_2(U_q^k)+f(x_q,t_k,U_q^k)\tag{16}$$

where it can be expanded as in Equation (17):

$$\begin{aligned}
&T_1\left(U_q^{(k+1)}\right)=\frac{1}{L}\sum_{p=0}^{L}\left[\frac{b_1(\mu_p)(\Delta t)^{-\mu_p}}{\Gamma(2-\mu_p)}\right.\\
&+\frac{b_2(\nu_p)(\Delta t)^{-\nu_p}}{\Gamma(3-\nu_p)}U_q^{(k+1)}+\frac{\kappa(\Delta x)^{-\alpha}}{2\Gamma(\alpha)\Gamma(3-\alpha)\cos\left(\frac{\pi\alpha}{2}\right)}\\
&\times\left\{\sum_{i=0}^{q-1}\left(U_{q-i+1}^{(k)}-2U_{q-i}^{(k)}+U_{q-i-1}^{(k)}\right)\left[(i+1)^{2-\alpha}-i^{2-\alpha}\right]\right.\\
&\left.\left.+\sum_{i=0}^{M-q-1}\left(U_{q+i-1}^{(k)}-2U_{q+i}^{(k)}+U_{q+i+1}^{(k)}\right)\left[(i+1)^{2-\alpha}-i^{2-\alpha}\right]\right\}\right.
\end{aligned}\tag{17}$$

and Equation (18):

$$\begin{aligned}
&T_2(U_q^k)=\frac{1}{L}\sum_{p=0}^{L}\left[b_1(\mu_p)\frac{(\Delta t)^{-\mu_p}}{\Gamma(2-\mu_p)}+b_2(\nu_p)\frac{(\Delta t)^{-\nu_p}}{\Gamma(3-\nu_p)}\right]U_q^k\\
&+\frac{1}{L}\sum_{p=0}^{L}b_2(\nu_p)(\frac{(\Delta t)^{-\nu_p}}{\Gamma(3-\nu_p)}(U_q^k-U_q^{k-1})\\
&-\frac{1}{L}\sum_{p=0}^{L}b_1(\mu_p)(\frac{(\Delta t)^{-\mu_p}}{\Gamma(2-\mu_p)}\sum_{j=1}^{k-1}(U_q^{k-j+1}-U_q^{k-j}))((j+1)^{1-\mu_p}\\
&-j^{1-\mu_p}))-\frac{1}{L}\sum_{p=0}^{L}b_2(\nu_p)(\frac{(\Delta t)^{-\nu_p}}{\Gamma(3-\nu_p)}\sum_{j=1}^{k-1}(U_q^{k-j+1}-2U_q^{k-j}\\
&+U_q^{k-j-1})((j+1)^{2-\nu_p}-j^{2-\nu_p}))-\frac{\kappa(\Delta x)^{-\alpha}}{2\Gamma(\alpha)\Gamma(3-\alpha)cos(\frac{\pi\alpha}{2})}\\
&\times\left\{\frac{(1-\alpha)(2-\alpha)U_0^k}{q^\alpha}+\frac{(2-\alpha)}{q^{\alpha-1}}(U_1^k-U_0^k)\right.\\
&\left.+\frac{(1-\alpha)(2-\alpha)U_M^k}{(M-q)^\alpha}-\frac{(2-\alpha)}{(M-q)^{\alpha-1}}(U_M^k-U_{M-1}^k)\right\}
\end{aligned}\tag{18}$$

Suppose the initial data has an error e_q^0 as in Equation (19)

$$\widetilde{\psi}_q^0=\psi(x_q)+e_q^0,\ q=1,\ldots,M\tag{19}$$

Let U_q^k and $\widetilde{U}_q^k$ are the solutions of Equations (14) and (15). Therefore, it can be depicted as in Equation (20)

$$T_1(e_q^{k+1})=T_2(e_q^k)+f(x_q,t_k,U_q^k)-f(x_q,t_k,\widetilde{U}_q^k)\tag{20}$$

in which $e_q^k=U_q^k-\widetilde{U}_q^k$. Also, let $E^k=[e_1^k,e_2^{k+1},\ldots,e_M^k]$, $k=0,1,2,\ldots,N$ and $\|E^k\|_\infty=\max_{1\le m\le M}|e_m^k|$. In proving the main theorems of this manuscript, we consider the following symbols in Equation (21):

$$\begin{aligned}
&\xi_1(L,\Delta t)=\frac{1}{L}\sum_{p=0}^{L}\frac{b_1(\mu_p)}{\Gamma(2-\mu_p)}(\Delta t)^{-\mu_p},\\
&\xi_2(L,\Delta t)=\frac{1}{L}\sum_{p=0}^{L}b_1(\mu_p)\frac{b_2(\nu_p)}{\Gamma(3-\nu_p)}(\Delta t)^{-\nu_p}
\end{aligned}\tag{21}$$

4.1. Theorem

Let $f(x,t,u)$ be a Lipschitz map. Then, the numerical method given by Equation (14) with initial boundary conditions Equation (15) is unconditionally stable, that is

$$\|E^n\|_\infty\le\varrho\,\|E^0\|_\infty,\ n=0,1,\ldots,N\tag{22}$$

where $\varrho>0$ and independent of the step sizes.

According to the conditions Equation (15), the inequality Equation (22) is satisfied for $n=0$. Suppose Equation (22) satisfies $n=1,\ldots,k$, assuming that $z\in\{1,2,\ldots,M\}$ such that $|e_z^{k+1}|=$

$\max_{0\le m\le M}|e_m^{k+1}| = \| E_z^{k+1} \|_\infty$, then, we have Equation (23):

$$
\begin{aligned}
&(\xi_1(L,\Delta t)+\xi_2(L,\Delta t)) \parallel E^{k+1} \parallel_\infty \\
&= (\xi_1(L,\Delta t)+\xi_2(L,\Delta t))|e_z^{k+1}| + \frac{\kappa(\Delta x)^{-\alpha}}{2\Gamma(\alpha)\Gamma(3-\alpha)cos(\frac{\pi\alpha}{2})} \\
&\times \left\{ \sum_{i=0}^{q-1} (2|e_{z-i}^k| - 2|e_{z-i}^k|)[(i+1)^{2-\alpha} - i^{2-\alpha}] \right. \\
&+ \left. \sum_{i=0}^{M-q-1} (2|e_{z+i}^k| - 2|e_{z+i}^k|)[(i+1)^{2-\alpha} - i^{2-\alpha}] \right\} \\
&\le (\xi_1(L,\Delta t)+\xi_2(L,\Delta t))|e_z^{k+1}| + \frac{\kappa(\Delta x)^{-\alpha}}{2\Gamma(\alpha)\Gamma(3-\alpha)cos(\frac{\pi\alpha}{2})} \\
&\times \{ \sum_{i=0}^{q-1} (2|e_{z-i}^k| - |e_{z-i-1}^k - |e_{z-i+1}^k|[(i+1)^{2-\alpha} - i^{2-\alpha}]) \\
&+ \sum_{i=0}^{M-q-1} (2|e_{z+i}^k| - |e_{z+i-1}^k| - |e_{z+i+1}^k|) \times [(i+1)^{2-\alpha} - i^{2-\alpha}] \} \\
&\le |(\xi_1(L,\Delta t)+\xi_2(L,\Delta t))|e_z^{k+1}| - \frac{\kappa(\Delta x)^{-\alpha}}{2\Gamma(\alpha)\Gamma(3-\alpha)cos(\frac{\pi\alpha}{2})} \\
&\times \{ \sum_{i=0}^{q-1} (|e_{z-i+1}^k| - 2|e_{z-i}^k| + |e_{z-i-1}^k|)[(i+1)^{2-\alpha} - i^{2-\alpha}] \\
&+ \sum_{i=0}^{M-q-1} (|e_{z+i+1}^k| - 2|e_{z+i}^k| + |e_{z+i-1}^k|)[(i+1)^{2-\alpha} - i^{2-\alpha}] \}| \\
&\le |(\xi_1(L,\Delta t)+\xi_2(L,\Delta t))|e_z^{k+1}| + \frac{\kappa(\Delta x)^{-\alpha}}{2\Gamma(\alpha)\Gamma(3-\alpha)cos(\frac{\pi\alpha}{2})} \\
&\times \left| \left\{ \sum_{i=0}^{q-1} (|e_{z-i+1}^k| - 2|e_{z-i}^k| + |e_{z-i-1}^k|) \times [(i+1)^{2-\alpha} - i^{2-\alpha}] \right. \right. \\
&+ \left. \left. \sum_{i=0}^{M-q-1} (|e_{z+i+1}^k| - 2|e_{z+i}^k| + |e_{z+i-1}^k|) \times [(i+1)^{2-\alpha} - i^{2-\alpha}] \right\} \right| \\
&= |T_1(e_z^{k+1})| = |T_2(e_z^k) + f(x_z,t_k,U_z^k) - f(x_z,t_k,\widetilde{U}_z^k)| \\
&\le |T_2(e_z^k)| + |f(x_z,t_k,U_z^k) - f(x_z,t_k,\widetilde{U}_z^k)|
\end{aligned}
\tag{23}
$$

Then, we have Equation (24)

$$
(\xi_1(L,\Delta t)+\xi_2(L,\Delta t)) \parallel E^{k+1} \parallel_\infty \le |T_2(e_z^k)| + L_f|U_z^k - \widetilde{U}_z^k)| \tag{24}
$$

where $L_f \in (0,1)$. Substituting Equation (18) into Equation (24) yields Equation (25)

$$
\begin{aligned}
&(\xi_1(L,\Delta t)+\xi_2(L,\Delta t)) \parallel E^{k+1} \parallel_\infty \le \sum_{j=1}^{k-1} a \parallel E^{k-j+1} \parallel_\infty \\
&+ b \parallel E^{k-j} \parallel_\infty + c \parallel E^{k-j-1} \parallel_\infty
\end{aligned}
\tag{25}
$$

where for $j=1$, we have Equation (26):

$$
\begin{aligned}
&a = (\xi_1 k^{1-\mu_p} + \xi_2 k^{2-\nu_p} + \xi_1 + 2\xi_2 + W(M,\alpha,z)), \\
&W(M,\alpha,z) = \left| \frac{\kappa(\Delta x)^{-\alpha}}{2\Gamma(\alpha)\Gamma(3-\alpha)cos(\frac{\pi\alpha}{2})} \right| \\
&\left\{ \frac{(1-\alpha)(2-\alpha)}{q^\alpha} + \frac{2(2-\alpha)}{q^{\alpha-1}} + \frac{(1-\alpha)(2-\alpha)}{(M-q)^\alpha} \right. \\
&\left. - \frac{2(2-\alpha)}{(M-q)^{\alpha-1}}, b = (\xi_1 k^{1-\mu_p} + 2\xi_2 k^{2-\nu_p} + \xi_2 + L_f), \right. \\
&c = \xi_2 k^{2-\nu_p}
\end{aligned}
\tag{26}
$$

and for $j = 2,\dots,k-1$, we have Equation (27):

$$
\begin{aligned}
a &= \xi_1 k^{1-\mu_p} + \xi_2 k^{2-\nu_p}, \\
b &= \xi_1 k^{1-\mu_p} + 2\xi_2 k^{2-\nu_p}, \\
c &= \xi_2 k^{2-\nu_p}
\end{aligned}
\tag{27}
$$

Equation (25) can also be rewritten as follows Equation (28)

$$
\begin{aligned}
&\parallel E^{k+1} \parallel_\infty \le \frac{1}{\xi_1(L,\Delta t)+\xi_2(L,\Delta t)} \sum_{j=1}^{k-1} a \parallel E^{k-j+1} \parallel_\infty \\
&+ b \parallel E^{k-j} \parallel_\infty + c \parallel E^{k-j-1} \parallel_\infty \\
&\le \frac{1}{\xi_1(L,\Delta t)+\xi_2(L,\Delta t)} (ak\delta_1 + bk\delta_2 + ck\delta_3) \parallel E^0 \parallel_\infty
\end{aligned}
\tag{28}
$$

From Equation (28), we get Equation (29):

$$
\parallel E^{k+1} \parallel_\infty \le \varrho \parallel E^0 \parallel_\infty \tag{29}
$$

where $\varrho = \max\{\frac{1}{\xi_1(L,\Delta t)+\xi_2(L,\Delta t)}(ak\delta_1 + bk\delta_2 + ck\delta_3)\}$. Thus, for each arbitrary initial rounding error E^0, there exists $\varrho > 0$, independent of L, Δt, and Δx, such that in Equation (30):

$$
\parallel E^n \parallel_\infty \le \varrho \parallel E^0 \parallel_\infty \tag{30}
$$

Therefore, our numerical method is unconditionally stable.

Suppose that the exact and approximate solutions of Equation (1) are U_q^k and $\widetilde{U}_q^k$, respectively. Then, we consider the error function at $(x_q,t_k$ by the following formula in Equation (31):

$$
e_q^k = U_q^k - \widetilde{U}_q^k,\ k = 1,\dots,N,\ q = 1,\dots,M \tag{31}
$$

in which $e^k = [e_1^k, e_2^k, \dots, e_M^k]$. Due to Equations (2) and (15), we have $e^0 = [0,0,\dots,0]$. Then, from Equation (14), we have Equation (32):

$$\frac{1}{L}\sum_{p=0}^{L} b_1(\mu_p)(\frac{(\Delta t)^{-\mu_p}}{\Gamma(2-\mu_p)}\sum_{j=0}^{k-1}(U_q^{k-j+1}-U_q^{k-j}))$$
$$\times((j+1)^{1-\mu_p}-j^{1-\mu_p})+b_1^{\mu_p}(\Delta t)^{2-\mu_p}\frac{\partial^2 U(x_q,\eta_k)}{\partial t^2})$$
$$-\frac{h^2}{24}F''_1(\mu)+\frac{1}{L}\sum_{p=0}^{L} b_2(\nu_p)(\frac{(\Delta t)^{-\nu_p}}{\Gamma(3-\nu_p)}\sum_{j=0}^{k-1}(U_q^{k-j+1}$$
$$-2U_q^{k-j}+U_q^{k-j-1})((j+1)^{2-\nu_p}-j^{2-\nu_p})$$
$$+b_2^{\nu_p}\frac{(\Delta t)^{4-\nu_p}}{24}\frac{\partial^4 U(x_q,\eta'_k)}{\partial t^4})-\frac{h^2}{24}F''_2(\nu))$$
$$=-\frac{\kappa(\Delta x)^{-\alpha}}{2\Gamma(\alpha)\Gamma(3-\alpha)cos(\frac{\pi\alpha}{2})}\{\frac{(1-\alpha)(2-\alpha)U_0^k}{q^\alpha}$$
$$+\frac{(2-\alpha)}{q^{\alpha-1}}(U_1^k-U_0^k)+\sum_{i=0}^{q-1}(U_{q-i+1}^k-2U_{q-i}^k$$
$$+U_{q-i-1}^k)[(i+1)^{2-\alpha}-i^{2-\alpha}]+\frac{(1-\alpha)(2-\alpha)U_M^k}{(M-q)^\alpha}$$
$$-\frac{(2-\alpha)}{(M-q)^{\alpha-1}}(U_M^k-U_{M-1}^k)+\sum_{i=0}^{M-q-1}(U_{q+i-1}^k$$
$$-2U_{q+i}^k+U_{q+i+1}^k)[(i+1)^{2-\alpha}-i^{2-\alpha}]\}$$
$$+b^\alpha\frac{(\Delta t)^{4-\alpha}}{24}\frac{\partial^4 U}{\partial x^4}(\theta_q,\eta_k)$$
$$+f(x_q,t_k,U_q^k)+\Delta t[\frac{\partial f}{\partial t}(x_q,\zeta_{k+1},U(x_q,\zeta_{k+1}))$$
$$+\frac{\partial f}{\partial U}(x_q,\zeta_{k+1},U(x_q,\zeta_{k+1}))\frac{\partial U}{\partial t}(x_q,\zeta_{k+1})] \tag{32}$$

in which $\eta_k \in (0,t_k)$, $\eta'_k \in (0,t_k)$, $\theta_q \in (x_{q-1},x_q)$ and $\zeta_k \in (t_k,t_{k+1})$. We can rewrite Equation (14) as follows in Equation (33):

$$\frac{1}{L}\sum_{p=0}^{L} b_1(\mu_p)(\frac{(\Delta t)^{-\mu_p}}{\Gamma(2-\mu_p)}\sum_{j=0}^{k-1}(U_q^{k-j+1}-U_q^{k-j}))$$
$$\times((j+1)^{1-\mu_p}-j^{1-\mu_p})+\frac{1}{L}\sum_{p=0}^{L} b_2(\nu_p)(\frac{(\Delta t)^{-\nu_p}}{\Gamma(3-\nu_p)}$$
$$\times\sum_{j=0}^{k-1}(U_q^{k-j+1}-2U_q^{k-j}+U_q^{k-j-1})((j+1)^{2-\nu_p}-j^{2-\nu_p})$$
$$+\frac{\kappa(\Delta x)^{-\alpha}}{2\Gamma(\alpha)\Gamma(3-\alpha)\cos(\frac{\pi\alpha}{2})}\{\frac{(1-\alpha)(2-\alpha)U_0^k}{q^\alpha}+\frac{(2-\alpha)}{q^{\alpha-1}}$$
$$\times(U_1^k-U_0^k)+\sum_{i=0}^{q-1}(U_{q-i+1}^k-2U_{q-i}^k+U_{q-i-1}^k)$$
$$\times[(i+1)^{2-\alpha}-i^{2-\alpha}]+\frac{(1-\alpha)(2-\alpha)U_M^k}{(M-q)^\alpha}-\frac{(2-\alpha)}{(M-q)^{\alpha-1}}$$
$$\times(U_M^k-U_{M-1}^k)+\sum_{i=0}^{M-q-1}(U_{q+i-1}^k-2U_{q+i}^k+U_{q+i+1}^k)$$
$$\times[(i+1)^{2-\alpha}-i^{2-\alpha}]\}=-\frac{1}{L}\sum_{p=0}^{L} b_1(\mu_p)b_1^{\mu_p}(\Delta t)^{2-\mu_p}$$
$$\times\frac{\partial^2 u(x_q,\eta_k)}{\partial t^2}+\frac{h^2}{24}F''_1(\mu)-\frac{1}{L}\sum_{p=0}^{L} b_2(\nu_p)b_2^{\nu_p}\frac{(\Delta t)^{4-\nu_p}}{24}$$
$$\times\frac{\partial^4 U(x_q,\eta'_k)}{\partial t^4}+\frac{h^2}{24}F''_2(\nu)+b^\alpha\frac{(\Delta t)^{4-\alpha}}{24}\frac{\partial^4 U}{\partial x^4}(\theta_q,\eta_k)$$
$$+f(x_q,t_k,U_q^k)+\Delta t[\frac{\partial f}{\partial t}(x_q,\zeta_{k+1},U(x_q,\zeta_{k+1}))$$
$$+\frac{\partial f}{\partial U}(x_q,\zeta_{k+1},U(x_q,\zeta_{k+1}))\frac{\partial U}{\partial t}(x_q,\zeta_{k+1})] \tag{33}$$

Applying the definition of T_1 and T_2, we can rewrite Equation (33) as in Equation (34):

$$T_1(U_q^{k+1})=T_2(U_q^k)+f(x_q,t_k,U_q^k)$$
$$-\frac{1}{L}\sum_{p=0}^{L} b_1(\mu_p)b_1^{\mu_p}(\Delta t)^{2-\mu_p}\frac{\partial^2 u(x_q,\eta_k)}{\partial t^2}$$
$$+\frac{h^2}{24}F''_1(\mu)-\frac{1}{L}\sum_{p=0}^{L} b_2(\nu_p)b_2^{\nu_p}\frac{(\Delta t)^{4-\nu_p}}{24}$$
$$\times\frac{\partial^4 U(x_q,\eta'_k)}{\partial t^4}+\frac{h^2}{24}F''_2(\nu)$$
$$+b^\alpha\frac{(\Delta x)^{4-\alpha}}{24}\frac{\partial^4 U}{\partial x^4}(\theta_q,\eta_k)$$
$$+\Delta t[\frac{\partial f}{\partial t}(x_q,\zeta_{k+1},U(x_q,\zeta_{k+1}))$$
$$+\frac{\partial f}{\partial U}(x_q,\zeta_{k+1},U(x_q,\zeta_{k+1}))\frac{\partial U}{\partial t}(x_q,\zeta_{k+1})] \tag{34}$$

Thus, the error e_q^k for $q=1,\ldots,M$ and $k=1,\ldots,N$ satisfies Equation (35)

$$\begin{cases} e_q^0=0, \\ T_1\left(U_q^{(k+1)}\right)=T_2\left(U_q^k\right)+\mathbb{R}_q^{(k+1)}+f(x_q,t_k,U_q^k)-f(x_q,t_k,\tilde{U}_q^k) \end{cases} \tag{35}$$

in which it can be defined as in Equation (36)

$$\mathbb{R}_q^{k+1}=-\frac{1}{L}\sum_{p=0}^{L} b_1(\mu_p)b_1^{\mu_p}(\Delta t)^{2-\mu_p}\frac{\partial^2 u(x_q,\eta_k)}{\partial t^2}$$
$$+\frac{h^2}{24}F''_1(\mu)-\frac{1}{L}\sum_{p=0}^{L} b_2(\nu_p)b_2^{\nu_p}\frac{(\Delta t)^{4-\nu_p}}{24}\frac{\partial^4 U(x_q,\eta'_k)}{\partial t^4}$$
$$+\frac{h^2}{24}F''_2(\nu)+b^\alpha\frac{(\Delta x)^{4-\alpha}}{24}\frac{\partial^4 U}{\partial x^4}(\theta_q,\eta_k)$$
$$+\Delta t[\frac{\partial f}{\partial t}(x_q,\zeta_{k+1},U(x_q,\zeta_{k+1}))$$
$$+\frac{\partial f}{\partial U}(x_q,\zeta_{k+1},U(x_q,\zeta_{k+1}))\frac{\partial U}{\partial t}(x_q,\zeta_{k+1})] \tag{36}$$

Consider $R^{k+1}=[\mathbb{R}_1^{k+1},\mathbb{R}_2^{k+1},\ldots,\mathbb{R}_M^{k+1}]$, $k=0,1,\ldots$. From Equation (37), we get

$$
\begin{aligned}
|\mathbb{R}_q^{k+1}| &\le P_1\frac{1}{L}\sum_{p=0}^{L} b_1(\mu_p)b_1^{\mu_p}(\Delta t)^{2-\mu_p} + P_2h^2 \\
&+ P_3\frac{1}{L}\sum_{p=0}^{L} b_2(\nu_p)b_2^{\nu_p}(\Delta t)^{4-\nu_p} + P_4h^2 \\
&+ P_5 b^{\alpha}(\Delta t)^{4-\alpha} + P_6\Delta t \\
&\le \bar{b}_1P_1 \max_{\mu\in(0,1)}\{b_1(\mu)\}(\Delta t)^{2-\mu_L} + P_2h^2 \\
&+ \bar{b}_2P_3 \max_{\nu\in(1,2)}\{b_2(\nu)\}(\Delta t)^{4-\nu_L} + P_4h^2 \\
&+ P_5\bar{b}^{\alpha}(\Delta t)^{4-\alpha} + P_6\Delta t
\end{aligned} \tag{37}
$$

in which it can be defined as in Equation (38):

$$
\begin{aligned}
&P_1 = \max_{t\in[0,T]}|\frac{\partial^2 u(x_q,t)}{\partial t^2}|, \quad P_2 = \max_{\mu\in(0,1)}|F''_1|, \\
&P_3 = \max_{t\in[0,T]}|\frac{1}{24}\frac{\partial^4 U(x_q,t)}{\partial t^4}|, \quad P_4 = \max_{\nu\in(1,2)}|F''_2|, \\
&P_5 = \frac{1}{24}\max_{x\in[0,L]}|\frac{\partial^4 U}{\partial x^4}(x,t_k)|, \\
&P_6 = \max_{\zeta_{k+1}\in[t_k,t_{k+1}]}|\{\frac{\partial f}{\partial t}(x_q,\zeta_{k+1},U(x_q,\zeta_{k+1})) \\
&\quad + \frac{\partial f}{\partial U}(x_q,\zeta_{k+1},U(x_q,\zeta_{k+1}))\frac{\partial U}{\partial t}(x_q,\zeta_{k+1})\}|, \\
&\bar{b}_1 = \max_p\{b_1^{\mu_p}\}, \quad \bar{b}_2 = \max_p\{b_2^{\nu_p}\}
\end{aligned} \tag{38}
$$

and $\bar{b}_\alpha = \max_\alpha\{b^\alpha\}$. Then, we get Equation (39):

$$
\begin{aligned}
&\| \mathbb{R}^{k+1} \|_\infty \le \mathbb{C}((\Delta t)^{2-\mu_L} + h^2 + (\Delta t)^{4-\nu_L} \\
&+ (\Delta t)^{4-\alpha} + (\Delta t))
\end{aligned} \tag{39}
$$

where $\mathbb{C} = \max\{\bar{b}_1P_1, P_2, \bar{b}_2P_3, P_4, \bar{b}^\alpha P_5, P_6, \}$.

5. Illustrative examples

Some numerical examples are demonstrated in this part to show the effectiveness of the studied numerical approach. The absolute errors for these illustrative examples at different points (x,t) are computed as follows in Equation (40):

$$
\begin{aligned}
&|e(x_q,t_k)| = |u(x_q,t_k) - u_q^k|, \\
&k = 1,\dots,N,\ q = 1,\dots,M,
\end{aligned} \tag{40}
$$

in which $u(x_q,t_k)$ and u_q^k show the exact and approximate solutions, respectively. Additionally, all numerical simulations presented in this study were conducted using Mathematica software (version 11). The computations were performed on a laptop equipped with an Intel Core i5 processor (2.40 GHz) and 16.00 GB of RAM. Moreover, the following formula Equation (41) was used to calculate the convergence order:

$$
\begin{aligned}
Rate_h &= \log_2(\frac{e(h,\Delta t)}{e(\frac{h}{2},\Delta t)}), \\
Rate_{\Delta t} &= \log_2(\frac{e(h,\Delta t)}{e(h,\frac{\Delta t}{2})}).
\end{aligned} \tag{41}
$$

5.1. Example 1

Consider Equation (42):

$$
\begin{aligned}
&\int_0^1 \Gamma(5-\mu)\,{}^C D_t^\mu u(x,t)d\mu \\
&+ \int_1^2 \Gamma(5-\nu)\,{}^C D_t^\nu u(x,t)d\nu = \\
&- (-\Delta)^{\frac{\alpha}{2}}u(x,t) + u^2(x,t) + g(x,t)
\end{aligned} \tag{42}
$$

where in Equation (43):

$$
\begin{aligned}
&g(x,t) = 24(x(1-x))^3\frac{(t^4-t^2)}{\ln t} - t^8(x(1-x))^6 \\
&+ g_1(x,t)g_1(x,t) = (2\cos(\frac{\alpha\pi}{2}))^{-1}t^4 \\
&\times\Bigg[\frac{\Gamma(4)}{\Gamma(4-\alpha)}(x^{3-\alpha}+(1-x)^{3-\alpha}) \\
&- \frac{3\Gamma(5)}{\Gamma(5-\alpha)}(x^{4-\alpha}+(1-x)^{4-\alpha}) \\
&+ \frac{3\Gamma(6)}{\Gamma(6-\alpha)}(x^{5-\alpha}+(1-x)^{5-\alpha}) \\
&-\frac{\Gamma(7)}{\Gamma(7-\alpha)}(x^{6-\alpha}+(1-x)^{6-\alpha})\Bigg]
\end{aligned} \tag{43}
$$

with conditions in Equation (44):

$$
\begin{aligned}
&u(x,0) = 0,\ x\in(0,1), \\
&u(0,t) = 0,\ u(1,t) = 0,\ t\in(0,1]
\end{aligned} \tag{44}
$$

The exact solution is $u(x,t) = t^4(x(1-x))^3$. We solved this problem using the numerical method developed in this study. The method was applied with $L = 20$, $M = N = 30$, and various values of α. Figure 1 presents the approximate solutions obtained by our method for these parameter values and different choices of α. This figure provides a visual representation of how the solution evolves across the spatial domain and time for different choices of α, offering insight into the influence of the fractional order on the overall behavior of the solution. Figure 2 compares the exact solution with the approximate solution at $L = 20$, $M = N = 30$, and various choices of α in $u(x,0.5)$. Figure 3 illustrates the absolute error functions for $L = 20$, $M = N = 30$, and various choices of α. These graphs illustrate the

discrepancy between the approximate and exact solutions, providing a clear indication of the accuracy of the numerical method. The absolute error is an essential metric for evaluating the effectiveness of the approximation, and these graphs help to assess how errors vary as α changes. Figure 4 shows the absolute error functions at $t = 0.5$ for the same values of L, M, and N with different choices of α. This figure focuses on the error at a specific time, offering more detailed insight into the temporal behavior of the numerical approximation. It is particularly useful for understanding how the error behaves at different fractional orders at a fixed point in time. Tables 1 and 2 provide the maximum errors and convergence orders for the numerical method in space and time, respectively. These tables are essential for understanding the accuracy and convergence behavior of the method. Specifically, the convergence order indicates how quickly the numerical solution approaches the exact solution as the grid resolution increases, and the maximum errors give a measure of the overall deviation from the true solution.

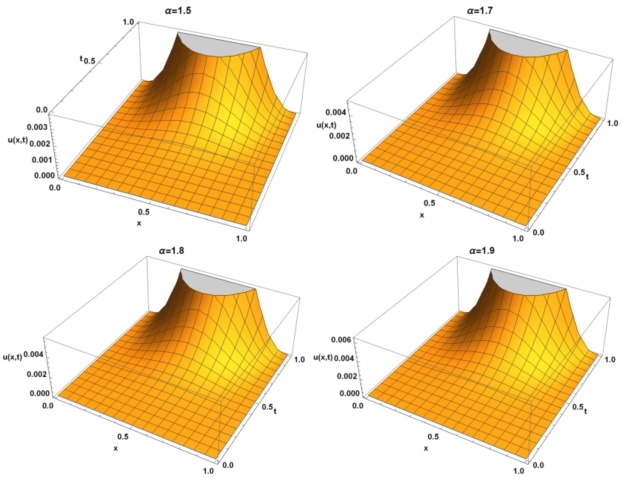

Figure 1. The plot of the approximate solution $u(x,t)$ with $L = 20$, $M = N = 30$, and various choices of α for Example 1

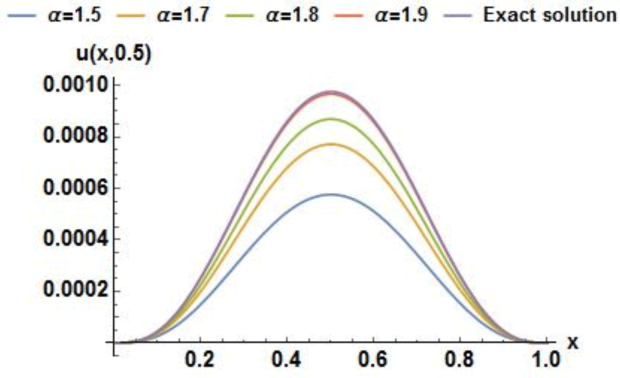

Figure 2. Approximate and exact solutions with $L = 20$, $M = N = 30$ and various choices of α for Example 1 when $t = 0.5$

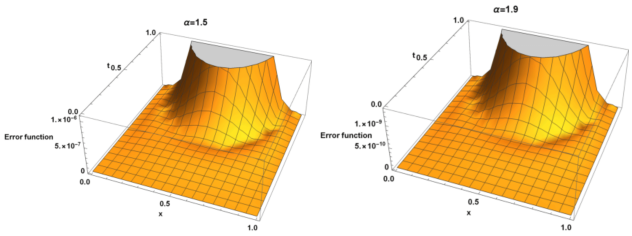

Figure 3. The absolute error functions with $L = 20$, $M = N = 30$ and various choices of α for Example 1

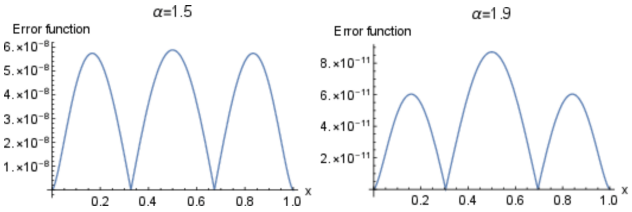

Figure 4. The absolute error functions with $L = 20$, $M = N = 30$ and various choices of α for Example 1 at $t = 0.5$

5.2. Example 2

Consider the problem in Equation (45)‘:

$$\int_0^1 \Gamma(\frac{7}{2}-\mu)\,{}^C D_t^{\mu} u(x,y,t)d\mu + \int_1^2 \Gamma(\frac{7}{2}-\nu)\,{}^C D_t^{\nu} u(x,y,t)d\nu = -(-\Delta)^{\frac{\alpha}{2}} u(x,y,t) + g(x,y,t) + \frac{15\sqrt{\pi}\sqrt{t}}{8lnt} \times (t^2-1)(x(1-x)y(1-y))^3,\ n \in \mathbb{N} \tag{45}$$

in which in Equation (46):

$$g(x,y,t) = (2cos(\frac{\alpha\pi}{2}))^{-1} t^{\frac{5}{2}}((1-y)y)^3 \times [\frac{\Gamma(4)}{\Gamma(4-\alpha)}(x^{3-\alpha}+(1-x)^{3-\alpha}) - \frac{3\Gamma(5)}{\Gamma(5-\alpha)}(x^{4-\alpha}+(1-x)^{4-\alpha}) + \frac{3\Gamma(6)}{\Gamma(6-\alpha)}(x^{5-\alpha}+(1-x)^{5-\alpha}) - \frac{\Gamma(7)}{\Gamma(7-\alpha)}(x^{6-\alpha}+(1-x)^{6-\alpha})] + (2cos(\frac{\beta\pi}{2}))^{-1} t^{\frac{5}{2}}((1-x)x)^3[\frac{\Gamma(4)}{\Gamma(4-\beta)}(y^{3-\beta} + (1-y)^{3-\beta}) - \frac{3\Gamma(5)}{\Gamma(5-\beta)}(y^{4-\beta}+(1-y)^{4-\beta})$$

Table 1. Comparison of the error function and convergence order with N= 100 for Example 1

M	$\alpha = 1.5$		$\alpha = 1.8$		$\alpha = 1.9$	
	$e(h, \Delta t)$	Rate_h	$e(h, \Delta t)$	Rate_h	$e(h, \Delta t)$	Rate_h
32	2.550426e-10	-	5.474700e-10	-	8.682241e-10	-
64	8.150868e-11	1.9820	1.558595e-10	1.9788	2.358879e-10	1.9863
128	1.205352e-11	1.9984	3.065866e-11	1.9980	5.072403e-11	1.9970
256	4.701125e-12	1.9937	1.034642e-11	1.9970	1.436730e-11	1.9972

Table 2. Comparison of the error function and convergence order with M= 100 for Example 1

N	$\alpha = 1.5$		$\alpha = 1.8$		$\alpha = 1.9$	
	$e(h, \Delta t)$	$\text{Rate}_{\Delta t}$	$e(h, \Delta t)$	$\text{Rate}_{\Delta t}$	$e(h, \Delta t)$	$\text{Rate}_{\Delta t}$
32	1.104018e-10	-	1.002382e-10	-	7.008703e-11	-
64	3.047415e-11	1.9900	2.438518e-11	1.8808	2.011908e-11	1.9931
128	6.557025e-12	1.9949	5.282357e-12	1.8845	5.045536e-12	1.9954
256	1.804933e-12	2.0007	1.500711e-12	1.8868	1.267602e-12	1.9928

$$+\frac{3\Gamma(6)}{\Gamma(6-\beta)}(y^{5-\beta}+(1-y)^{5-\beta}) - \frac{\Gamma(7)}{\Gamma(7-\beta)}(y^{6-\beta}+(1-y)^{6-\beta})] \tag{46}$$

in which $(x,t) \in [0,1]\times[0,1]$ under the conditions in Equation (47):

$$\begin{aligned} &u(x,y,0) = 0,\ (x,y) \in (0,1)\times(0,1),\\ &u(x,y,t) = 0, (x,y) \in \partial((0,1)\times(0,1)) \end{aligned} \tag{47}$$

The exact solution for this model is given by $u(x,t) = t^{\frac{5}{2}}(x(1-x)y(1-y))^3$. Applying our numerical method, taking $L = 20$ and $M = N = 30$, the numerical results for this example for different values of α are shown in Figure 5 if $t = 0.5$. The absolute error functions with $L = 20$, $M = N = 30$, and various choices of α for this example at $t = 0.5$ are demonstrated in Figure 6.

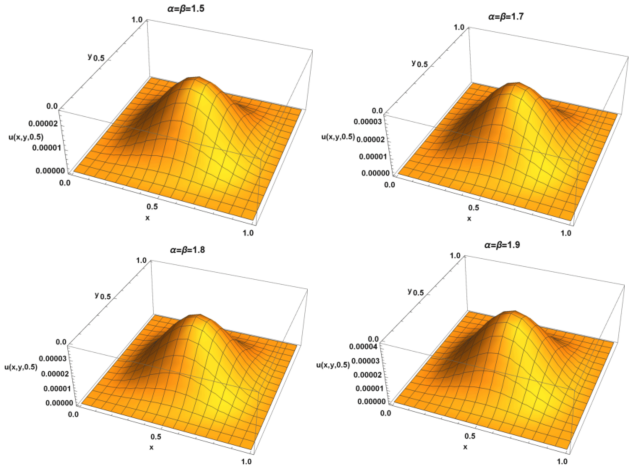

Figure 5. The plot of the approximate solution $u(x,t)$ with $L = 20$, $M = N = 30$ and various choices of α for Example 2

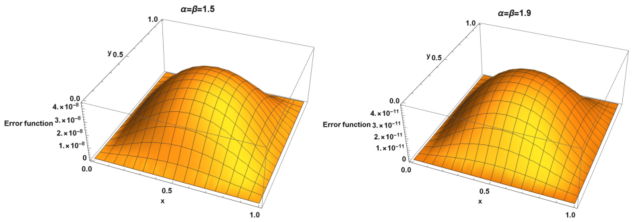

Figure 6. The absolute error functions with $L = 20$, $M = N = 30$ and various choices of α for Example 2

5.3. Example 3

Consider the time-fractional reaction-diffusion model of distributed order with$h$ $\alpha = 2$ in Equation (48):

$$\int_0^1 \Gamma(\frac{7}{2}-\mu)\,{}^C D_t^{\mu} u(x,t)d\mu = u_{xx}(x,t) + u^2(x,t) + \frac{15\sqrt{\pi}t\sqrt{t}}{8lnt}(t-1)(x(1-x)) - 2t^5 - (xt(1-x))^2 \tag{48}$$

with the following conditions in Equation (49):

$$u(x,0) = u(0,t) = u(1,t) = 0,\ x \in (0,1),\ t \in (0,1] \tag{49}$$

The exact solution for this model was calculated in previous studies [30, 31] by $u(x,t) = t^{\frac{5}{2}}x(x-1)$. We solved this model using the studied method on the domains $x \in (0,1)$ and $t \in (0,1]$ when $\Delta x = h$. Figure 7 shows the numerical results for different values of $\Delta x = h$. Figure 8 reports the error function for different values of h. Figure 9 shows the error function for different values of h with $t = 0.5$. We compared the method presented in this study with the methods discussed in previous articles[46,47] based on the error function. The comparison results are summarized in Table 3, which also includes the

Table 3. Comparison of the maximum errors and convergence orders with $\Delta t = (\Delta x)^2$ for Example 3

$\Delta x = h$	Reference[30]		Reference[31]		Proposed method	
	$e(h, \Delta t)$	$\text{Rate}_{\Delta t}$	$e(h, \Delta t)$	$\text{Rate}_{\Delta t}$	$e(h, \Delta t)$	$\text{Rate}_{\Delta t}$
0.5	7.43e-2	-	2.45e-2	-	1.34e-7	-
0.25	3.22e-2	0.60	5.47e-3	1.08	4.36e-8	1.99
0.125	8.99e-3	0.92	1.30e-3	1.04	1.21e-8	1.78
0.0625	2.31e-3	0.98	3.20e-4	1.01	2.13e-9	1.73

convergence order for the proposed method. This table provides a comprehensive overview of the performance of the proposed method in relation to those from previous studies, highlighting the accuracy and convergence behavior.

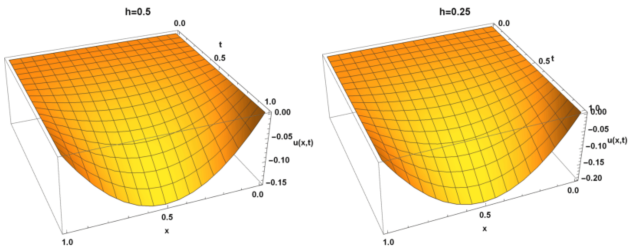

Figure 7. The surface of the approximate solution $u(x, t)$ with $L = 20$, $M = N = 30$ and various choices of α for Example 3

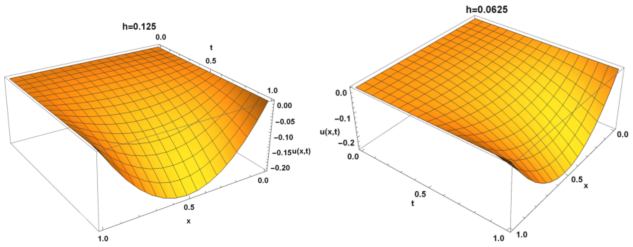

Figure 8. The absolute error functions with $L = 20$, $M = N = 30$, and various choices of α for Example 3

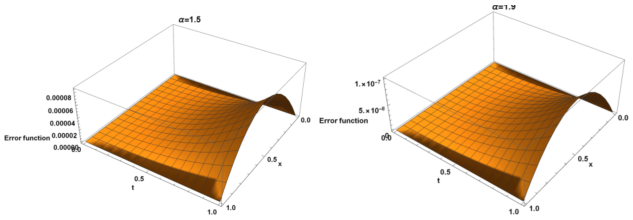

Figure 9. The absolute error functions with $L = 20$, $M = N = 30$ and various choices of α for Example 3 at $t = 0.5$

6. Conclusion

In this study, we analyzed the distributed-order multi-dimensional time-fractional telegraph equations, incorporating Caputo time- and Riesz space-fractional derivatives. The finite difference method was employed to approximate the Riesz space-fractional derivative with respect to the spatial variable. To approximate the distributed-order fractional operator, we applied the midpoint method to discretize the integral term, followed by the use of the finite difference method to approximate the Caputo fractional derivative with respect to the time variable. We have rigorously proved the convergence and stability of the proposed numerical method. To demonstrate the high efficiency and accuracy of the method, we conducted several numerical experiments, comparing the results with those obtained from other numerical methods found in the literature. The comparison clearly shows that the proposed method outperforms existing approaches in terms of both efficiency and performance, making it a highly effective tool for solving distributed-order time-fractional telegraph equations.

Acknowledgments

None.

Funding

The work was supported by the University of Tabriz, Iran (Grant No. 2070).

Conflict of interest

The authors declare that they have no competing interests.

Author contributions

Conceptualization: Safar Irandoust Pakchin, Mohammad Hossein Derakhshan
Data curation: Mohammad Hossein Derakhshan
Investigation: All authors
Methodology: All authors
Software: All authors
Writing – original draft: Shahram Rezapour
Writing – review & editing: All authors

Availability of data

All data analyzed and generated have been included in the manuscript.

AI tools statement

All authors confirm that no AI tools were used in the preparation of this manuscript.

References

1. Azroul E, Kamali N, Ragusa MA, Shimi M. Variational methods for a p(x,.)-fractional bi-nonlocal problem of elliptic type. *Rend Circ Mat Palermo, II. Ser.* 2025;74(1):1-21. https://doi.org/10.1007/s12215-024-01156-7
2. Alotaibi M, Jleli M, Ragusa MA, Samet B. On the absence of global weak solutions for a nonlinear time-fractional SchrÑ†dinger equation. *Appl Anal.* 2024;103(1):1-15. https://doi.org/10.1080/00036811.2022.2036335
3. Kilbas AA, Srivastave HM, Trujillo JJ. *Theory and Applications of Fractional Differential Equations.* Amsterdam: Elsevier B.V.; 2006. ISBN:0444518320, 9780444518323
4. Podlubny I. *Fractional Differential Equations: An Introduction to Fractional Derivatives, Fractional Differential Equations, to Methods of Their Solution and Some of their Applications*, vol. 198. New York: Academic Press; 1998. ISBN:0080531989, 9780080531984
5. Mollahasani N, Moghadam MM, Afrooz K. A new treatment based on hybrid functions to the solution of telegraph equations of fractional order. *Appl Math Model.* 2016; 40(4):2804-2814. https://doi.org/10.1016/j.apm.2015.08.020
6. Wang R, Shi L, Wang B. Asymptotic behavior of fractional nonclassical diffusion equations driven by nonlinear colored noise on R^N. *Nonlinearity.* 2019; 32(11): 4524-4556. https://doi.org/10.1088/1361-6544/ab32d7
7. Yasin F, Afzal Z, Saleem MS, Jahangir N, Shang Y. Hermite–Hadamard type inequality for non-convex functions employing the Caputo–Fabrizio fractional integral. *Res Math.* 2024;11(1):2366164. https://doi.org/10.1080/27684830.2024.2366164
8. Mohammed AA, Marasi HR, Derakhshan MH, Kumar P. An efficient numerical method for the time-fractional distributed order nonlinear Klein-Gordon equation with shifted fractional Gegenbauer multi-wavelets method. *Phys Scr.* 2023;98:084001. https://doi.org/10.1088/1402-4896/accedb
9. Umarov S. Continuous time random walk models associated with distributed order diffusion equations. *Fract Cal Appl Anal.* 2015;18:821-837. https://doi.org/10.1515/fca-2015-0049
10. Guo S, Mei L, Zhang Z. Time-fractional Gardner equation for ion-acoustic waves in negative-ion-beam plasma with negative ions and non-thermal nonextensive electrons. *Phys Plasmas.* 2015;22:052306. https://doi.org/10.1063/1.4919264
11. Ansari A, Derakhshan MH, Askari H. Distributed order fractional diffusion equation with fractional Laplacian in axisymmetric cylindrical configuration. *Commun Nonlinear Sci Numer Simul.* 2022;113:106590. https://doi.org/10.1016/j.cnsns.2022.106590
12. Derakhshan MH. Existence, uniqueness, Ulam-Hyers stability and numerical simulation of solutions for variable order fractional differential equations in fluid mechanics. *J Appl Math Comput.* 2022;68(1):403-429. https://doi.org/10.1007/s12190-021-01537-6
13. Irandoust-pakchin S, Abdi-mazraeh S, Fahimi-khalilabad I. Higher order class of finite difference method for time-fractional Liouville-Caputo and space-Riesz fractional diffusion equation. *Filomat.* 2024;38(2):505-521. https://doi.org/10.2298/FIL2402505I
14. Irandoust-Pakchin S, Abdi-Mazraeh S, Khani A. Numerical solution for a variable-order fractional nonlinear cable equation via Chebyshev cardinal functions. *Comput Math and Math Phys.* 2017;57:2047-2056. https://doi.org/10.1134/S0965542517120120
15. Fahimi-khalilabad I, Irandoust-pakchin S, Abdi-mazraeh S. High-order finite difference method based on linear barycentric rational interpolation for Caputo type sub-diffusion equation. *Math Comput Simulat.* 2022;199:60-80. https://doi.org/10.1016/j.matcom.2022.03.008
16. Caputo M. Mean fractional-order-derivatives differential equations and filters. *Ann Univ Ferrara.* 1995;41:73-84. https://doi.org/10.1007/BF02826009
17. Caputo M. Distributed order differential equations modelling dielectric induction and diffusion. *Fract Calc Appl Anal.* 2001;4:421-442. ww.math.bas.bg/fcaa, www.diogenes.bg/fcaa.
18. Caputo M. Diffusion with space memory modelled with distributed order space fractional differential equations. *Ann Geophys.* 2003;46(2). https://doi.org/10.4401/ag-3395
19. Chechkin A, Gorenflo R, Sokolov I. Retarding subdiffusion and accelerating superdiffusion governed by distributed-order fractional diffusion equations. *Phys Rev E.* 2002;66:046129. https://doi.org/10.1103/PhysRevE.66.046129
20. Sokolov I, Chechkin A, Klafter J. Distributed-order fractional kinetics. *Acta Physica Polonica B.* 2004;35:1323-1341. https://doi.org/10.48550/arXiv.cond-mat/0401146
21. Vieira N, Rodrigues MM, Ferreira M. Time-fractional telegraph equation of distributed order in higher dimensions. *Commun Nonlinear Sci Numer Simul.* 2021;102:105925. https://doi.org/10.1016/j.cnsns.2021.105925
22. Ratner V, Zeevi YY. Denoising-enhancing images on elastic manifolds. *IEEE Trans Image Process.* 2011;20(8):2099-2109. https://doi.org/10.1109/TIP.2011.2118221
23. Gorenflo R, Luchko Y, Stojanovi *M*. Fundamental solution of a distributed order time-fractional diffusion-wave equation as probability density. *Fract Calc Appl Anal.* 2013;16(2):297-316. https://doi.org/10.2478/s13540-013-0019-6

24. Mainardi F, Pagnini G. The role of the Fox-Wright functions in fractional sub-diffusion of distributed order. *J Comput Appl Math.* 2007;207(2):245-257. https://doi.org/10.1016/j.cam.2006.10.014
25. Ahmed HF, Moubarak MRA, Hashem WA. Gegenbauer spectral tau algorithm for solving fractional telegraph equation with convergence analysis. *Pramana - J Phys.* 2021;95(2):1-16. https://doi.org/10.1007/s12043-021-02113-0
26. Zhang Y, Qian J, Papelis C, Sun P, Yu Z. Improved understanding of bimolecular reactions in deceptively simple homogeneous media: from laboratory experiments to Lagrangian quantification. *Water Resour Res.* 2014;50(2):1704-1715. https://doi.org/10.1002/2013WR014711
27. Sun HG, Chen W, Li C, Chen YQ. Fractional differential models for anomalous diffusion. *Physica A: Stat Mech Appl.* 2010;389(14):2719-2724. https://doi.org/10.1016/j.physa.2010.02.030
28. Gao GH, Sun ZZ. Two difference schemes for solving the one-dimensional time distributed-order fractional wave equations. *Numer Algorithms.* 2017;74:675-697. https://doi.org/10.1007/s11075-016-0167-y
29. Wang Z, Vong S. Compact difference schemes for the modified anomalous fractional sub-diffusion equation and the fractional diffusion-wave equation. *J Comput Phys.* 2014;277:1-15. https://doi.org/10.1016/j.jcp.2014.08.012
30. Ye H, Liu F, Anh V, Turner I. Numerical analysis for the time distributed-order and Riesz space fractional diffusions on bounded domains. *IMA J Appl Math.* 2015;80(3):825-838. https://doi.org/10.1093/imamat/hxu015
31. Jian HY, Huang TZ, Gu XM, Zhao YL. Fast second-order implicit difference schemes for time distributed–order and Riesz X.L. space fractional diffusion–wave equations. *Comput Math Appl.* 2021;94:136-154. https://doi.org/10.1016/j.camwa.2021.05.003
32. Kharazmi E, Zayernouri M, Karniadakis G. Petrov-Galerkin and spectral collocation methods for distributed order differential equations. *SIAM J Sci Comput.* 2017;39:A1003-A1037. https://doi.org/10.1137/16M1073121
33. Gao G, Sun Z. Two alternating direction implicit difference schemes with the extrapolation method for the two-dimensional distributed-order differential equations. *Comput Math Appl.* 2015;69: 926-948. https://doi.org/10.1016/j.camwa.2015.02.023
34. Duong P, Kwok E, Lee M. Deterministic analysis of distributed order systems using operational matrix. *Appl Math Model.* 2016;40:1929-1940. https://doi.org/10.1016/j.apm.2015.09.035
35. Mashayekhi S, Razzaghi M. Numerical solution of distributed order fractional differential equations by hybrid functions. *J Comput Phys.* 2016;315:169-181. https://doi.org/10.1016/j.jcp.2016.01.041
36. Abbaszadeh M, Dehghan M. Meshless upwind local radial basis function-finite difference technique to simulate the time-fractional distributed-order advection-diffusion equation. *Eng Comput.* 2021;37:873-889. https://doi.org/10.1007/s00366-019-00861-7
37. Ye H, Liu F, Anh V. Compact difference scheme for distributed-order time-fractional diffusion-wave equation on bounded domains. *J Comput Phys.* 2015;298:652-660. https://doi.org/10.1016/j.jcp.2015.06.025
38. Chen H, LÃ¼ S, Chen W. Finite difference/spectral approximations for the distributed order time fractional reaction-diffusion equation on an unbounded domain. *J Comput Phys.* 2016;315:84-97. https://doi.org/10.1016/j.jcp.2016.03.044
39. Qiu W, Xu D, Chen H, Guo J. An alternating direction implicit Galerkin finite element method for the distributed-order time-fractional mobile-immobile equation in two dimensions. *Comput Math Appl.* 2020;80(12):3156-3172. https://doi.org/10.1016/j.camwa.2020.11.003
40. Yang Z, Zheng X, Wang H. A variably distributed-order time-fractional diffusion equation: analysis and approximation. Comput *Methods Appl Mech Eng.* 2020;367:113118. https://doi.org/10.1016/j.cma.2020.113118
41. Abdelkawy MA, Lopes AM, Zaky MA. Shifted fractional Jacobi spectral algorithm for solving distributed order time-fractional reaction-diffusion equations. *Comput Appl Math.* 2019;38:1-21. https://doi.org/10.1007/s40314-019-0845-1
42. Ansari A, Derakhshan MH. On spectral polar fractional Laplacian. *Math Comput Simul.* 2023;206:636-663. https://doi.org/10.1016/j.matcom.2022.12.008
43. Derakhshan MH, Aminataei A. A numerical method for finding solution of the distributed-order time-fractional forced Kortewegde Vries equation including the Caputo fractional derivative. *Math Methods Appl Sci.* 2022;45(5):3144-3165. https://doi.org/10.1002/mma.7981
44. Ahmed HF, Hashem WA. Improved Gegenbauer spectral tau algorithms for distributed-order time-fractional telegraph models in multi-dimensions. *Numer Algorithms.* 2023; 93(3):1013-1043. https://doi.org/10.1007/s11075-022-01452-2
45. Ilic M, Liu F, Turner I, Anh V. Numerical approximation of a fractional-in-space diffusion equation, I. *Fract Calc Appl Anal.* 2005;8(3):323-341. http://eudml.org/doc/11303
46. Morgado ML, Rebelo M. Numerical approximation of distributed order reaction-diffusion equations. *J Appl Math Comput.* 2015; 275:216-227. https://doi.org/10.1016/j.cam.2014.07.029
47. Moghaddam BP, Tenreiro Machado JA, Morgado ML. Numerical approach for a class of distributed

order time fractional partial differential equations. *Appl Numer Math.* 2019;136:152-162. https://doi.org/10.1016/j.apnum.2018.09.019

Safar Irandoust Pakchin*, after the completing his Ph.D. in Mathematics at the Faculty of Mathematics, Statistics and Computer Sciences, University of Tabriz, Iran, in July 2012, he engaged as an Assistant Professor at Department of Applied Mathematics, Faculty of Mathematics, Statistics and Computer Sciences, University of Tabriz, Iran, in February 2013 until now. His research areas include partial differential equations, fractional differential equations, fractional stochastic integro-differential equations, and image and signal processing. He has developed spectral methods, especially wavelets, and fractional linear multistep methods.*
http://orcid.org/0000-0001-9548-4762

Mohammad Hossein Derakhshan *holds a Ph.D. and five postdoctoral degrees from K. N. Toosi University of Technology and University of Tabriz. His expertise lies in numerical analysis and differential equations, and he has successfully completed advanced courses in these fields. Dr. Derakhshan applies mathematical modeling, numerical methods, and differential equations, especially in fractional-order and distributed-order systems, to solve complex scientific and engineering problems.*
https://orcid.org/0000-0001-6464-7338

Shahram Rezapour *is a professor of mathematics at Azarbaijan Shahid Madani University, Tabriz, Iran, and holds a visiting professor position at China Medical University, Taichung, Taiwan. He also held an eminent scholarship position at Kyung Hee University, Seoul, Republic of Korea, in 2023.*
http://orcid.org/0000-0003-3463-2607

An International Journal of Optimization and Control: Theories & Applications
(https://accscience.com/journal/ijocta)